J Math Chem (2011) 49:2013–2031
DOI 10.1007/s10910-011-9872-x

ORIGINAL PAPER

The numerical simulation of vanadium RedOx flow batteries

I. M. Bayanov · R. Vanhaelst

Received: 22 March 2011 / Accepted: 21 June 2011 / Published online: 1 July 2011

Abstract In this article a theoretical model of a RedOx flow cell (RFC), based on an equation system of fluid dynamics and of electrochemistry, is presented. A numerical algorithm of the solution of the equation system is developed. The results of numerical simulation of processes in the RFC are analyzed and validated in a test cell. The effects of different electrode collectors and current densities on the operation of the RFC are studied.

Keywords RedOx flow · Numerical simulation · Vanadium

1 Introduction

The modeling of operation of RFC is very attractive theoretical problem due to complex of partial differential equations of fluid dynamics and of electrochemistry. A solution of this problem can allow optimizing a configuration and parameters of RFC and parameters of electrolytes.

The RedOx flow batteries (RFB) are used as efficient new energy storage for a wide range of applications [1], for example, solar power plants and wind power plants. Recent decades all vanadium RedOx flow battery (VRB) is considered as the most suitable large scale energy storage system due its advantageous properties such as high energy efficiency (more than 80%), long operation time, and low cost. The VRB

I. M. Bayanov (✉)
Kazan State Technical University, Karl Marx str. 10, 420111 Kazan, Russian Federation
e-mail: bim1966@mail.ru

R. Vanhaelst
University of Applied Sciences Ostfalia, Kleiststr. 14-16, 38440 Wolfsburg, Germany
e-mail: r.vanhaelst@ostfalia.de

operation was firstly successfully demonstrated in the University of New South Wales (Australia) [2]. Using only vanadium species in both half-cells overcomes the problem of electrolytes cross contamination caused by the transfer of ions across the membrane.

These features of the VRB make very attractive its use in electric vehicles. However, its low energy density has restricted these capabilities. To overcome this limitation it is necessary to optimize the number of parameters of RFB, for example, increasing the concentration of the vanadium ions in the solution [3], using of other Redox couples [4] or optimizing the configuration of the VRB [5].

The optimization of VRB operation can be carried out on the basis of theoretical modeling and numerical simulation [5–7]. These models conclude the equation systems, which are solved numerically only. It carried out using standard computer codes (for, example, COMSOL Multiphysics package). But this problem can be solved by means of relatively simple methods of numerical modeling [8,9]. It makes possible to control the accuracy of calculations, to optimize the space and time steps etc.

In this article the numerical simulation of operation of RFC on the basis of numerical methods is realized.

2 The theoretical model of RedOx flow cell (RFC)

2.1 Operation of RFC

The scheme of RFC is presented in Fig. 1. Each half-cell consists of porous graphite electrode and is restricted by graphite plate from one side and ion-exchange membrane from other side. Positive and negative electrolytes, stored in external tanks, are pumped through the half-cells. The electrochemical interaction between electrolytes is carried out by means of H^+-ion exchange across the membrane. The reduction and oxidation reactions take place in half-cells by discharge process:

in positive half-cell

$$VO_2^+ + 2H^+ + e^- \rightarrow VO^+ + H_2O,$$

in negative half-cell

$$V^{2+} \rightarrow V^{3+} + e^-.$$

Here V^{2+}, V^{3+}, VO^+, VO_2^+ are the vanadium ions with different valence, labeled in following text as V^{2+}, V^{3+}, V^{4+}, V^{5+}.

The processes in the RFC are described by the equations of fluid mechanics, electrodynamics and electrochemistry. The flow of electrolyte through the porous electrodes and diffusion of ions across the membrane can be modeled by the conservation laws of mass, of momentum, and of energy. The distribution of electric potential in RFC can be obtained by solving of Poison equations. The electrochemical interaction of species in the cell is described by the Nernst equation and by the Butler–Volmer law. An interference of these processes makes the solution of equations complicate. But

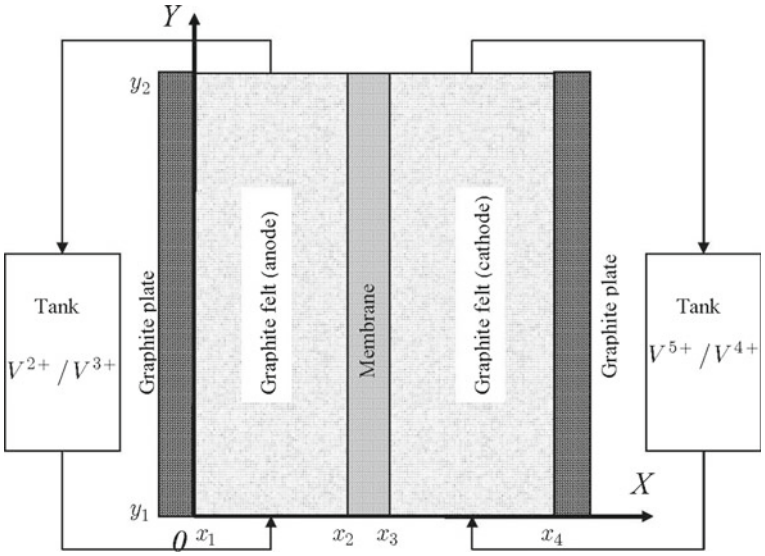

Fig. 1 The structure of a test cell

the solution can be separated in several stages because of different time scales t_i of the processes.

The electrolyte flow in cell can be considered as a stationary fluid dynamics problem ($t_1 \to \infty$), an electric field in electrolyte and electrode system is established with the speed of light ($t_2 \to 0$), the changes of the chemical composition in cell take place by flowing of electrolyte through the cell ($t_2 = L/v$) where L is a length of cell, v is a speed of flow in cell.

2.2 Fluid dynamics equations

We suppose that the electrolyte is noncompressible liquid. The first stage of solving the problem is based on conservation law of mass for noncompressible liquid

$$div\,\overrightarrow{v} = 0 \tag{1}$$

A flow velocity $\overrightarrow{v}$ in porous electrode is determined by Darcy's law

$$\overrightarrow{v} = -\frac{k}{\mu\epsilon} grad p, \tag{2}$$

where p is a pressure, k is the permeability, ϵ is the porosity, μ is the dynamic viscosity.

The permeability of the porous electrode is calculated by Carman–Kozeny equation [10]

$$k = \frac{d_f^2 \epsilon^2}{16 k_C K (1-\epsilon^2)}.$$

A combination of these expressions gives the Laplace equation for pressure

$$\frac{\partial^2 p}{\partial x^2} + \frac{\partial^2 p}{\partial y^2} = 0. \tag{3}$$

The boundary conditions for the pressure in the half-cell can be written as follows:
for $x = x_1$ and $x = x_2$

$$\frac{\partial p}{\partial y} = 0 \tag{4}$$

for $y = y_1$

$$p = p_{in}$$

for $y = y_2$

$$p = p_{out}.$$

The distribution of the pressure $p = p(x, y)$ is obtained by solving the Eq. (3) with boundary conditions (4) and the distribution of velocity $\vec{v} = \vec{v}(x, y)$ is determined by expression (2).

The second stage of solving the problem describes the convective and diffusive transfer of ions in cell

$$div(m_p c_k \vec{v}) - D_{eff,k}\left(\frac{\partial^2 c_k}{\partial x^2} + \frac{\partial^2 c_k}{\partial y^2}\right) = J_k, k = 1, \ldots, N_{sp} \tag{5}$$

where c_k are molar concentrations of ions, $D_{eff,k}$ are effective diffusion coefficients, J_k are the rates of chemical reactions, N_{sp} is a number of species in electrolytes. The effective diffusion coefficient in liquids in porous media is smaller than in pure liquid and can be calculated by Bruggemann correction [11]

$$D_{eff,k} = \varepsilon^{3/2} D_k.$$

2.3 Equations of electrochemistry

In the third stage we shall obtain the rates of chemical reactions. The equations presented in this article are written for the discharge process in a RFC. An electrochemical process is determined by its current density j_i on the surface of the electrode

$$J_i = S_a j_i / F, \tag{6}$$

where F is Faraday number, S_a is specific surface area of porous electrode. The current densities is described by the Butler–Volmer law (for positive and negative electrode j_1, j_2, respectively)

$$
\begin{aligned}
j_1 &= j_{01}\left(\frac{c_{05}}{c_5}\exp\left(-\frac{0.5F\eta_1}{RT}\right) - \frac{c_{04}}{c_4}\exp\left(\frac{0.5F\eta_1}{RT}\right)\right),\\
j_2 &= j_{02}\left(\frac{c_{03}}{c_3}\exp\left(-\frac{0.5F\eta_2}{RT}\right) - \frac{c_{02}}{c_2}\exp\left(\frac{0.5F\eta_2}{RT}\right)\right),
\end{aligned}
\tag{7}
$$

where $j_{01} = k_1 F\sqrt{c_4 c_5}$, $j_{02} = k_2 F\sqrt{c_2 c_3}$ are the exchange current densities, c_{0k} are the concentrations of the species at the surface of the electrodes.

The over-potentials for positive and negative electrode reactions are defined as

$$
\begin{aligned}
\eta_1 &= \varphi_{S1} - \varphi_{l1} - E_1,\\
\eta_2 &= \varphi_{S2} - \varphi_{l2} - E_2,
\end{aligned}
\tag{8}
$$

where $\varphi_{S1}, \varphi_{S2}, \varphi_{l1}, \varphi_{l2}$ are the electric potentials in electrode (s) and electrolyte (l). The open circuit potentials are estimated from the Nernst equations

$$
\begin{aligned}
E_1 &= E_{01} + \tfrac{RT}{F}\ln\tfrac{c_5}{c_4},\\
E_2 &= E_{02} + \tfrac{RT}{F}\ln\tfrac{c_3}{c_2},
\end{aligned}
\tag{9}
$$

where E_{01}, E_{02} are equilibrium potentials.

The distribution of electric potentials $\varphi_{S1}, \varphi_{S2}, \varphi_{l1}, \varphi_{l2}$ can be found by solving the equation system

$$
\begin{aligned}
-\sigma_{eff}\nabla^2\varphi_{S1} &= aj_1,\\
-k_{eff1}\nabla^2\varphi_{l1} &= -aj_1,\\
-\sigma_{eff}\nabla^2\varphi_{S2} &= -aj_2,\\
-k_{eff2}\nabla^2\varphi_{l2} &= aj_2,
\end{aligned}
\tag{10}
$$

that was obtained from the Ohm's law. Here $\sigma_{eff}, k_{eff1}, k_{eff2}$ are the electric conductivities of porous electrode, of positive and of negative electrolytes, respectively. It should be noted that the right-hand sides of equations (10) contain the electric potentials due to the expressions (7) and (8).

The effective conductivity of porous electrodes is different from the conductivity of solid one and corrected by

$$
\sigma_{eff} = (1-\varepsilon)^{3/2}\sigma_s.
$$

The conductivities of electrolytes are calculated by [12]

$$
k_{eff} = \frac{F^2}{RT}\sum_k z_k^2 D_k c_k. \tag{11}
$$

Here z_k is a valence of ions.

The concentration values c_{0k} at the electrode surface can be determined by introducing the local mass transfer coefficients k_{m1}, k_{m2} that are calculated as

$$k_{m1} = k_{m2} = 1.6 \times 10^{-4} v^{0.4},$$

where v is a flow velocity.

The local flux of the species at the surface of the positive electrode during discharge will be

$$\begin{aligned} k_{m1}(c_{04} - c_4) &= k_1 \sqrt{c_4 c_5} \left(\frac{c_{04}}{c_4} \exp\left(\frac{0.5F\eta_1}{RT} \right) - \frac{c_{05}}{c_5} \exp\left(-\frac{0.5F\eta_1}{RT} \right) \right), \\ k_{m1}(c_{05} - c_5) &= k_1 \sqrt{c_4 c_5} \left(\frac{c_{05}}{c_5} \exp\left(-\frac{0.5F\eta_1}{RT} \right) - \frac{c_{04}}{c_4} \exp\left(\frac{0.5F\eta_1}{RT} \right) \right). \end{aligned} \quad (12)$$

The values c_{0i} have been obtained by solving of this equation system

$$\begin{aligned} c_{04} &= \frac{B_1 c_5 + (1 + B_1) c_4}{1 + A_1 + B_1}, \\ c_{05} &= \frac{A_1 c_4 + (1 + A_1) c_5}{1 + A_1 + B_1}, \end{aligned} \quad (13)$$

where A_1, B_1 are expressed as

$$\begin{aligned} A_1 &= \frac{k_1}{k_{m1}} \sqrt{\frac{c_5}{c_4}} \exp\left(\frac{0.5F\eta_1}{RT} \right), \\ B_1 &= \frac{k_1}{k_{m1}} \sqrt{\frac{c_4}{c_5}} \exp\left(-\frac{0.5F\eta_1}{RT} \right). \end{aligned} \quad (14)$$

The similar expressions can be obtained for negative half-cell coefficients c_{02} and c_{03}

$$\begin{aligned} c_{02} &= \frac{B_2 c_3 + (1 + B_2) c_2}{1 + A_2 + B_2}, \\ c_{03} &= \frac{A_2 c_2 + (1 + A_2) c_3}{1 + A_2 + B_2}, \end{aligned} \quad (15)$$

$$A_2 = \frac{k_2}{k_{m2}} \sqrt{\frac{c_3}{c_2}} \exp\left(\frac{0.5F\eta_2}{RT} \right),$$

$$B_2 = \frac{k_2}{k_{m2}} \sqrt{\frac{c_2}{c_3}} \exp\left(-\frac{0.5F\eta_2}{RT} \right). \quad (16)$$

2.4 Boundary conditions

We suppose that the membrane can only be penetrated by H^+-ions. Then the boundary conditions for the equations (5) are determined by the concentration values of H^+-ions ($k = 1, 6$) and of the vanadium ions ($k = 2, 3, 4, 5$)

for $x = x_1$

$$\frac{\partial c_1}{\partial x} = 0,$$

for $x = x_2$

$$\frac{\partial c_1}{\partial x} = -I/F,$$

for $x = x_3$

$$\frac{\partial c_6}{\partial x} = -I/F,$$

for $x = x_4$

$$\frac{\partial c_6}{\partial x} = 0,$$

for $x = x_1, x = x_2$

$$\frac{\partial c_2}{\partial x} = 0, \quad \frac{\partial c_3}{\partial x} = 0,$$

for $y = y_2$

$$\frac{\partial c_2}{\partial y} = 0, \quad \frac{\partial c_3}{\partial y} = 0,$$

for $x = x_3, x = x_4$

$$\frac{\partial c_4}{\partial x} = 0, \quad \frac{\partial c_5}{\partial x} = 0,$$

for $y = y_2$

$$\frac{\partial c_4}{\partial y} = 0, \quad \frac{\partial c_5}{\partial y} = 0,$$

for $y = y_1$

$$c_k = c_{in,k}, \tag{17}$$

where I is a current density on the surface of the membrane and of the graphite plate. The inlet concentrations of species $c_{in,k}$ are time depended due the change of state of charge (soc) during the operation of cell:

$$
\begin{aligned}
c_{in,1} &= c_{in,0},\\
c_{in,2} &= c_{in,V2} \cdot soc,\\
c_{in,3} &= c_{in,V3}(1 - soc),\\
c_{in,4} &= c_{in,V4}(1 - soc),\\
c_{in,5} &= c_{in,V5} \cdot soc,\\
c_{in,6} &= c_{in,0}.
\end{aligned}
$$

where $c_{in,0}, c_{in,V2}, c_{in,V3}, c_{in,V4}, c_{in,V5}$ are initial values of concentration of H^+, V^{2+}, V^{3+}, V^{4+}, V^{5+} -ions in tanks, respectively. The soc can be estimated as [5]

$$soc = 1 - \frac{c_{in,3}}{c_{in,V3}}.$$

The time dependency of the inlet concentrations of the species $c_{in,k}$ is determined by the equation [6]

$$\frac{dc_{in,k}}{dt} = \frac{Q}{V}(c_{out,k} - c_{in,k}),$$

where Q is volumetric flow rate, V is a volume of electrolyte in tank, $c_{out,k}$ are the outlet concentrations of species.

To solve the equation system (10) the boundary conditions for potentials are needed. For discharge process there are
for $x = x_1$

$$-\sigma_{eff}\frac{\partial \varphi_{S1}}{\partial x} = I, \quad -k_{eff1}\frac{\partial \varphi_{l1}}{\partial x} = 0,$$

for $x = x_2$

$$-\sigma_{eff}\frac{\partial \varphi_{S1}}{\partial x} = 0, \quad -k_{eff1}\frac{\partial \varphi_{l1}}{\partial x} = I,$$

for $x = x_3$

$$-\sigma_{eff}\frac{\partial \varphi_{S2}}{\partial x} = 0, \quad -k_{eff2}\frac{\partial \varphi_{l2}}{\partial x} = I,$$

for $x = x_4$

$$-\sigma_{eff}\frac{\partial \varphi_{S2}}{\partial x} = I, \quad -k_{eff2}\frac{\partial \varphi_{l2}}{\partial x} = 0,$$

for $y = y_1, y_2$

$$-\sigma_{eff}\frac{\partial \varphi_{S1}}{\partial y} = 0, \quad -k_{eff1}\frac{\partial \varphi_{l1}}{\partial y} = 0,$$

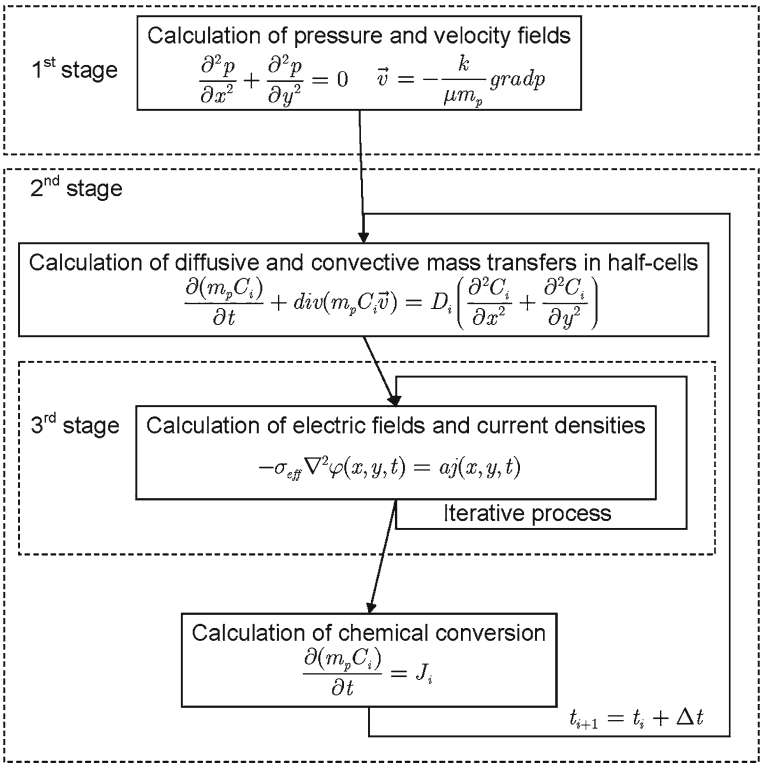

Fig. 2 The program flowchart of computer code

for $y = y_3, y_4$

$$-\sigma_{eff}\frac{\partial \varphi_{S2}}{\partial y}=0, \quad -k_{eff2}\frac{\partial \varphi_{l2}}{\partial y}=0. \tag{18}$$

3 Numerical solution of equation system

According to the concept of the different time scales of processes in RFC the solution of the problem includes three stages (Fig. 2) of finding of

- distribution of the pressure and of the flow velocity in cell,
- distribution of the chemical species in the cell taking into account electrochemical interaction,
- distribution of the electric field and of the current density in the cell.

3.1 Solution of Laplace equation for pressure field in half-cell

In the first stage we solve the equation (3) with boundary conditions (4) and find a pressure $p = p(x, y)$. In the simplest configuration of half-cell (Fig. 1) we have the

closed boundaries at the left and right sides and the open boundaries at bottom and upper sides. In this case the distribution of the pressure can be found analytically and it is linear

$$p = p_{in} + \frac{p_{out} - p_{in}}{L} \cdot y. \tag{19}$$

A distribution of velocity can be expressed by (2) and it is uniform

$$\vec{v} = \vec{v}_0 = -\frac{k}{\mu\epsilon} \cdot \frac{p_{out} - p_{in}}{L} \cdot \vec{e}_y, \tag{20}$$

where $\vec{e}_y$ is the unit vector along axis OY. For more complicate configurations of cell the solution can be obtained numerically. For it we use the iteration method of solution of Dirichlet's problem [13]. A rectangular computational grid with $(N_x \cdot N_y)$ points has space steps $\Delta x = \frac{d}{N_x}$ and $\Delta y = \frac{L}{N_y}$. The equation (3) is approximated by a difference equation

$$\frac{p_{i+1,j} - 2p_{i,j} + p_{i-1,j}}{(\Delta x)^2} + \frac{p_{i,j+1} - 2p_{i,j} + p_{i,j-1}}{(\Delta y)^2} = 0.$$

Then the value of grid function of pressure $p^n_{i,j}$ at the iteration step $(n+1)$ is

$$p^{n+1}_{i,j} = \frac{\left(p^n_{i+1,j} + p^n_{i-1,j}\right)(\Delta y)^2 + \left(p^n_{i,j+1} + p^n_{i,j-1}\right)(\Delta x)^2}{2\left((\Delta x)^2 + (\Delta y)^2\right)}. \tag{21}$$

The iteration process is stopped if an adequate accuracy is reached. The velocity distribution $\vec{v} = \vec{v}(x, y)$ is obtained by numerical differentiation on the basis of expression (2). We have found the distributions $p = p(x, y)$ for a number of cell configurations, but it is beyond of subject of this article. These solutions can be employed for the problem in 3D formulation.

3.2 Solution of system of diffusion equations

The second stage is connected with the solution of the equation system (5) with boundary conditions (17). There is a whole number of methods of computational fluid dynamics to solve this system. We used a method of coarse particles [8]. It is employed in wide range of problems of fluid mechanics and we had written a computer program on the basis of this method.

The domain of calculation is divided by the computational grid into $N = N_x \cdot N_y$ cells, which are the so-called coarse particles. The numerical algorithm at each time step Δt consists of three stages typical of the method of coarse particles. In these stages, the diffusive transport of mass and momentum (stage I) are successively taken into account to be followed by the convective transport of these quantities (stages II and III) with computed velocity $\vec{v} = \vec{v}(x, y)$.

At the first stage, the grid moves together with the substance, and there are no mass fluxes through cell boundaries. The coarse particles move due to a pressure gradient. The substance density remains unchanged. At this stage, intermediate values of concentration c are calculated:

$$\tilde{c}^n_{i,j} = c^n_{i,j} + A\left(c^n\right)\Delta t, \tag{22}$$

where the items $A(c^n) = A_1(c^n) + A_2(c^n)$ corresponding to diffusive transfer calculated as

$$A_1\left(c^n\right) = D\left(\frac{\left(c^n_{i+1,j} - c^n_{i,j}\right)}{\Delta x} - \frac{\left(c^n_{i,j} - c^n_{i-1,j}\right)}{\Delta x}\right)\frac{1}{\Delta x}, \tag{23}$$

$$A_2\left(c^n\right) = D\left(\frac{\left(c^n_{i,j+1} - c^n_{i,j}\right)}{\Delta y} - \frac{\left(c^n_{i,j} - c^n_{i,j-1}\right)}{\Delta y}\right)\frac{1}{\Delta y}. \tag{24}$$

At the second stage, the computational grid returns to the initial state, and mass fluxes Δm through cell boundaries are calculated:

$$\begin{aligned}\Delta m^n_{i+\frac{1}{2},j} &= \begin{cases} \rho^n_{i,j}\frac{(v_x)^n_{i,j}+(v_x)^n_{i+1,j}}{2}\Delta y_j\Delta t, & \text{if } (v_x)^n_{i,j} + (v_x)^n_{i+1,j} > 0 \\ \rho^n_{i+1,j}\frac{(v_x)^n_{i,j}+(v_x)^n_{i+1,j}}{2}\Delta y_j\Delta t, & \text{if } (v_x)^n_{i,j} + (v_x)^n_{i+1,j} < 0 \end{cases} \\ \Delta m^n_{i-\frac{1}{2},j} &= \ldots \end{aligned} \tag{25}$$

The fluxes of concentration Δc, which "move" together with the mass flux, are also calculated. For example, concentration fluxes through the right boundary of the cell of grid along the x axis are written in the form

$$\rho^n_{i+\frac{1}{2},j}\Delta c^n_{i+\frac{1}{2},j} = \Delta M^n_{i+\frac{1}{2},j}\cdot\tilde{c}^n_{i,j}, \tag{26}$$

At the third stage, we calculate the final values of concentration at the next time step:

$$\begin{aligned} c^{n+1}_{i,j} = {} & \frac{\rho^n_{i,j}}{\rho^{n+1}_{i,j}}\tilde{c}^n_{i,j} + \frac{1}{\rho^{n+1}_{i,j}\Delta x\Delta y} \\ & \times\left(\tilde{c}^n_{i-1,j}\Delta m^n_{i-\frac{1}{2},j} + \tilde{c}^n_{i,j-1}\Delta m^n_{i,j-\frac{1}{2}} - \tilde{c}^n_{i+1,j}\Delta m^n_{i+\frac{1}{2},j} - \tilde{c}^n_{i,j+1}\Delta m^n_{i,j+\frac{1}{2}}\right). \end{aligned} \tag{27}$$

This method is used by solution of wide range of fluid dynamics problems. For example, it is very easy to include in equation system the equation of thermoconductivity, and solution of it carried out by the same method as diffusion equation.

After these stages of method of coarse particles a distribution of electric field can be found. This stage is described in part 3.3.

After the calculation of electric field distribution in cell we find the current densities in half-cells by means of expressions (7). It allows calculating the chemical conversions (6) of species and the concentrations at the next time step

$$c_{i,j}^{n+1} = c_{i,j}^{n} + n_{st} \frac{S_a J_{i,j}}{F} \cdot \Delta t \tag{28}$$

where n_{st} is stoichiometric coefficient ($n_{st} = n_1, n_2, n_3, n_4, n_5$), $c_{i,j}^{n}$ is grid function of concentrations ($c = c_1, c_2, c_3, c_4, c_5, c_6$) at the time step n.

3.3 Solution of Dirichlet's problem for an electric field

The third stage of solution is realized after three stages of method of coarse particles at each time step. The system of equations (7)–(10) with boundary conditions (18) is solved by iteration method. First equation in the system (10) has a form

$$\nabla^2 \varphi_{S1} = F(\varphi_{S1}, \varphi_{l1}). \tag{29}$$

A difference scheme of equation for grid function of potential $\varphi_{i,j}$ can be written as [13]

$$\frac{\varphi_{i+1,j} - 2\varphi_{i,j} + \varphi_{i-1,j}}{(\Delta x)^2} + \frac{\varphi_{i,j+1} - 2\varphi_{i,j} + \varphi_{i,j-1}}{(\Delta y)^2} = F(\varphi_{S,i,j}, \varphi_{l,i,j}) \tag{30}$$

Here

$$\begin{aligned} \varphi_{i,j} &= (\varphi_{S1})_{i,j} \text{ or } (\varphi_{l1})_{i,j} \text{ or } (\varphi_{S2})_{i,j} \text{ or } (\varphi_{l2})_{i,j}, \\ \varphi_{S,i,j} &= (\varphi_{S1})_{i,j} \text{ or } (\varphi_{S2})_{i,j}, \\ \varphi_{l,i,j} &= (\varphi_{l1})_{i,j} \text{ or } (\varphi_{l2})_{i,j}, \end{aligned}$$

respectively.

To realize the iteration method an additive term is written in left-hand side of equation (29) that will go to zero by iteration cycle

$$\frac{\varphi_{i,j}^{n+1} - \varphi_{i,j}^{n}}{\tau} + \frac{\varphi_{i+1,j}^{n} - 2\varphi_{i,j}^{n} + \varphi_{i-1,j}^{n}}{(\Delta x)^2} + \frac{\varphi_{i,j+1}^{n} - 2\varphi_{i,j}^{n} + \varphi_{i,j-1}^{n}}{(\Delta y)^2} = F(\varphi_{S,i,j}^{n}, \varphi_{l,i,j}^{n}). \tag{31}$$

The value of function $\varphi_{i,j}^{n+1}$ at the next iteration step is expressed by the values of function at previous iteration step $\varphi_{i,j}^{n}$ from the algebraic equation

$$\varphi_{i,j}^{n+1} = \varphi_{i,j}^{n} + Q(\varphi_{i,j}^{n}) \cdot \tau, \tag{32}$$

where is iteration step and

$$Q(\varphi_{i,j}^n) = F(\varphi_{S,i,j}^n, \varphi_{l,i,j}^n) - \frac{\varphi_{i+1,j}^n - 2\varphi_{i,j}^n + \varphi_{i-1,j}^n}{(\Delta x)^2} - \frac{\varphi_{i,j+1}^n - 2\varphi_{i,j}^n + \varphi_{i,j-1}^n}{(\Delta y)^2}.$$

At the initial iteration step ($n = 0$) the functions have the values

$$\varphi_{S1}^{(0)} = E_1, \quad \varphi_{l1}^{(0)} = 0, \quad \varphi_{S2}^{(0)} = E_2, \quad \varphi_{l2}^{(0)} = 0. \tag{33}$$

Here E_1, E_2 are expressed by (9).

The equations (10) have on right-hand side an exponential function due the expressions (8) that complicates iterative convergence. Therefore the iteration step τ must have a small value. This requires a long computation time what can delay the calculations. To avoid it the calculation of electric field should not be carried out at each time step. This can be done because the change of potentials at this step is very small (for $\Delta t = 10^{-3}$ s relative change of potential is 10^{-8}). We calculated the electric potentials and current densities every 10^5-th time step. An electrochemical conversion of species between these steps is calculated by constant current densities with adequate accuracy.

4 Results

4.1 Initial parameters

The values of parameters, used in numerical simulations, are presented in Tables 1, 2, 3, 4, 5, 6.

Table 1 Constants

Parameter	Symbol	Value	Unit
Avogadro number	N_A	6.022×10^{23}	mol^{-1}
Faraday number	F	96350	C mol^{-1}
Universal gas constant	R	8.31	$\text{J mol}^{-1}\ \text{K}^{-1}$
Carman–Kozeny constant	k_{CK}	4.28	–

Table 2 Electrode properties

Parameter	Symbol	Value	Unit
Width	h	52×10^{-3}	m
Length	L	77×10^{-3}	m
Thickness	d	3×10^{-3}	m
Porosity	ϵ	0.929	–
Specific surface	S_a	1.62×10^4	m^2
Diameter of fiber	d_f	17.6×10^{-6}	m

Table 3 Membrane properties

Parameter	Symbol	Value	Unit
Thickness	d_m	1.25×10^{-4}	m
Diffusion coefficient of H^+-ion	$D_{H,m}$	3.5×10^{-10}	$m^2 s^{-1}$

Table 4 Electrolyte properties

Parameter	Symbol	Value	Unit
Viscosity	μ	4.928×10^{-3}	Pa s^{-1}
Diffusion coefficient	D_H	9.312×10^{-9}	m^2 s^{-1}
Diffusion coefficient	D_2	3.9×10^{-10}	m^2 s^{-1}
Diffusion coefficient	D_3	3.9×10^{-10}	m^2 s^{-1}
Diffusion coefficient	D_4	2.4×10^{-10}	m^2 s^{-1}
Diffusion coefficient	D_5	2.4×10^{-10}	m^2 s^{-1}
Initial concentration of vanadium (positive)	C_5	0.5	mol l^{-1}
Initial concentration of vanadium (negative)	C_2	0.5	mol l^{-1}
Initial concentration of H^+-ion (positive)	C_1	5	mol l^{-1}
Initial concentration of H^+-ion (negative)	C_0	5	mol l^{-1}

Table 5 Electrochemical properties

Parameter	Symbol	Value	Unit
Standard reaction rate (positive)	k_1	6.8×10^{-7}	m s^{-1}
Standard reaction rate (negative)	k_2	1.7×10^{-7}	m s^{-1}
Equilibrium potential	E_1	1.004	V
Equilibrium potential	E_2	−0.255	V
Stoichiometric coefficient	n_1	−2	–
Stoichiometric coefficient	n_2	−1	–
Stoichiometric coefficient	n_3	1	–
Stoichiometric coefficient	n_4	1	–
Stoichiometric coefficient	n_5	−1	–

Table 6 Operation parameters

Parameter	Symbol	Value	Unit
Temperature	T	300	K
Volume of electrolyte in each tank	V	0,1	l
Volumetric flow rate	Q	1.67×10^{-6}	m^3 s^{-1}

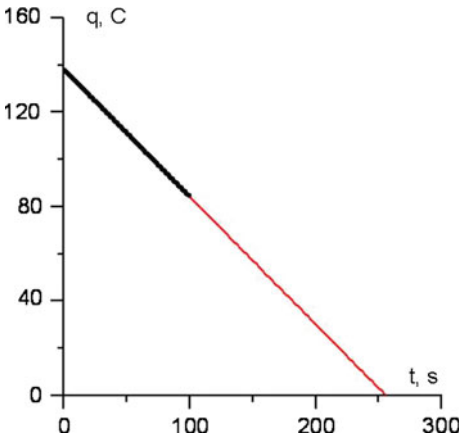

Fig. 3 Comparison of theoretical and of calculated values of charge in cell

4.2 Results of calculation

4.2.1 Validation of computer code

To validate the computer code at first the simplest case of operation of RFC was simulated. At zero flow velocity ($v = 0$) the charge capacity in cell is determined by volume of electrolyte in cell. A total charge in catolyte in initial state is determined by *soc* and concentration of V^{+5}-ions. It can be calculated as

$$q = F \int_V c(V^{5+}) dV, \tag{34}$$

where F is Faraday constant, V is volume of catolyte in cell. During a discharge by constant current the value of total charge fall linearly depended on time

$$q = q_0 - I \cdot t. \tag{35}$$

A value q_{calc} was calculated on the basis of expression (34) during a simulation and was compared with this expression (Fig. 3). There is a good agreement between theoretical and calculated values. This test checks the 1st and 2nd stages of calculation process (see Fig. 2). The precision of calculation of concentration is verified on the basis of conservation law of mass

$$Q = \sum_k Q_k = \sum_k \int_S M_k c_k v dS = const, \tag{36}$$

where Q is flow rate of electrolyte, M_k is molar masses of species with number k. A precision of calculation of electric potentials is defined by accuracy of iteration process. It was chosen 10^{-14}.

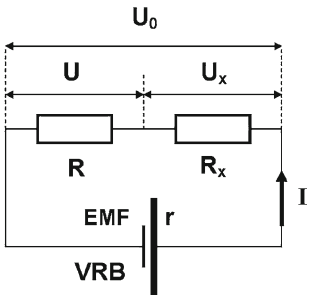

Fig. 4 Electric circuit of discharge setup

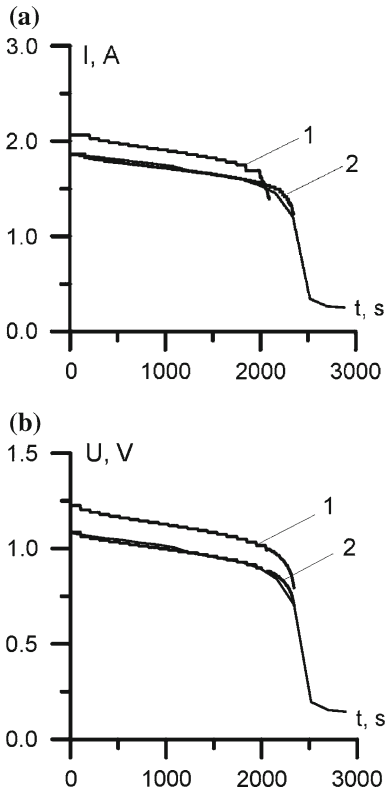

Fig. 5 Comparison of experimental and theoretical curves of current (**a**) and voltage (**b**) by resistance $R = 0.47\ \Omega$ for steel plates

4.2.2 The comparison with the experimental data

To validate the simulation results a test redox-flow cell was build. The structure of the cell is shown in Fig. 1. The cell consists of a positive and negative half-cell. Each half cell contains a graphite electrode and a graphite felt. They are separated by Nafion membrane. The electrolyte which is solved in two separate tanks is pumped through the cell by double-membrane pump. The flow velocity can be varied by the pump.

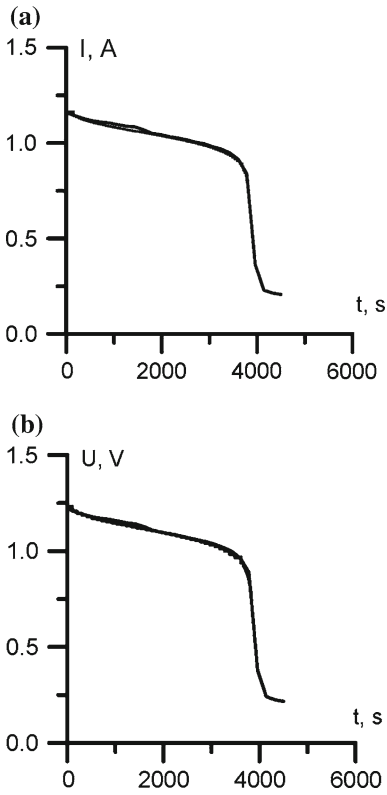

Fig. 6 Comparison of experimental and theoretical curves of current (**a**) and voltage (**b**) by resistance $R = 1.1\ \Omega$ for steel plates

The electrolyte solution 0.8M $VOSO_4$, 0.8M $V_2(SO_4)_3$, 0.05M H_3PO_4, 2M H_2SO_4 was used. In a first stage a pre-charging process was carried out. And than charge-discharge experiments were performed.

The charge was realized by constant voltage $U = 1.7$ V. The discharge took place by constant resistance with ratings $R = 0.47, 1.1\ \Omega$.

First row of experiments was performed using stainless steel plates as an current collector. Comparisons of results of numerical simulations with experimental data were provided by followed algorithm. Figure 5 demonstrates this algorithm for measurements by $R = 0.47\ \Omega$. In experiment the voltage and current were measured. The ratio of these quantities gives the real value of resistance $R = U/I = 0.584\ \Omega$. With this "measured" resistance R the simulation gives a curve that is not coincided with measured one (curve 1 in Fig. 5a). It can be explained by additional resistance R_x of electrode plates, connecting wires, and contacts (Fig. 4). Than the value of resistance $R_0 = R + R_x = 0.658\ \Omega$ for simulation was chosen for maximal coinciding of calculated and measured curves of current (curve 2 in Fig. 5a). Those, it gives the value of $R_x = R_0 - R = 0.074\ \Omega$. The calculated curve of voltage $U_0(t)$ (curve 1 in Fig. 5b) must be adjusted taking into account the losses at resistance R_x: $U = U_0 - R_x \cdot I$. The Fig. 5b shows a good coincidence of the curves (curve 2).

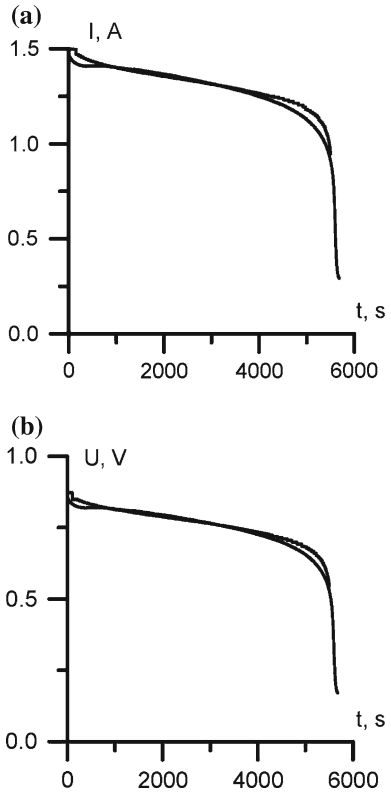

Fig. 7 Comparison of experimental and theoretical curves of current (**a**) and voltage (**b**) by resistance $R = 0.47\ \Omega$ for carbon plates

The same algorithm of comparison was used for the measurement with resistance value $R_0 = 1.1\ \Omega$ (Fig. 6). The value of $R_x = 0.061\ \Omega$ was obtained.

An internal resistance of cell consists of resistances of graphite felt, of electrolytes, and of membrane. It can be calculated also according to Ohm's law $r = EMF/I - R_0$. The values of $r = 0.080$ and $0.082\ \Omega$ were found for two measurements, respectively.

The second row of experiments was performed using carbon plates (Sigraflex) as an current collector. The comparison of experimental and theoretical curves for two cases ($R = 0.47, 1.1\ \Omega$) (Figs. 7, 8) gives the values of additional resistance $R_x = 0.297$ and $0.302\ \Omega$ that are four times more in comparison with values by steel plates. And the values of internal resistance $r = 0.074$ and $0.077\ \Omega$ were obtained. They are similar to the values that were obtained above.

5 Conclusion

In the article the theoretical model of the RFC is presented. On the basis of the model the numerical simulation of operation of the RFC is realized. The numerical solution of equations of fluid dynamics and of electrochemistry is carried out by means of the method of coarse particles combined by the iteration process. The analysis of

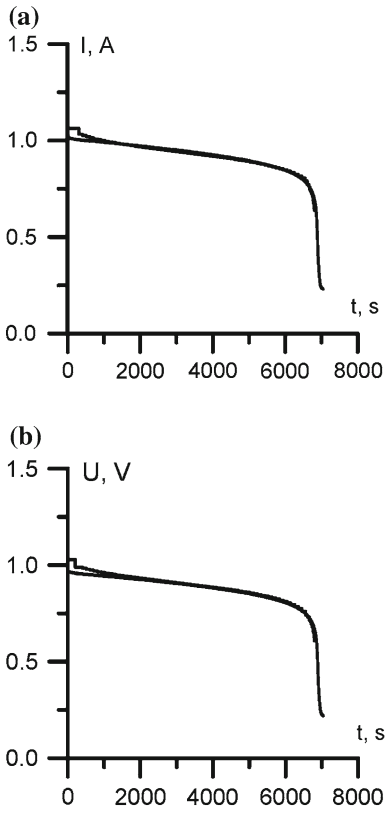

Fig. 8 Comparison of experimental and theoretical curves of current (**a**) and voltage (**b**) by resistance $R = 1.1\ \Omega$ for carbon plates

the calculation results combined with experimental data allows to obtain the main characteristics of the RFC—the voltage, the current and the internal resistance.

References

1. M. Skyllas-Kazacos, G. Kazacos, G. Poonl et al, Int. J. Energy Res. doi:10.1002/er.1658 (2009)
2. M. Skyllas-Kazacos, R.G. Robins, US Patent No. 4,786,567 (1986)
3. F. Rahman, M. Skyllas-Kazacos, J. Power Sources **189**, 1212 (2009)
4. M. Skyllas-Kazacos, J. Power Sources **124**, 299 (2003)
5. H. Al-Fetlawi, A.A. Shah, F.C. Walsh, Electrochim. Acta **55**, 78 (2009)
6. A.A. Shah, M.J. Watt-Smith, F.C. Walsh, Electrochim. Acta **53**, 8087 (2008)
7. D. Youa, H. Zhanga, J. Chena Electrochim. Acta **54**, 6827 (2009)
8. O.M. Belotserkovskii, Y.M. Davydov, Method of coarse particles in gas dynamics (in Russian). (Nauka, Moscow, 1982)
9. S.K. Godunov, V.C. Ryabenkii, Difference schemes. Introduction in theory (in Russian). (Nauka, Moscow, 1977)
10. M.M. Tomadakis, T.J. Robertson, J. Compos. Mater. **39**, 163 (2005)
11. M. Verbrugge, R.J. Hill, J. Elecrochem. Soc. **137**, 886 (1990)
12. D. Schmal, J. Van Erkel, P.J. Van Duin, J. Appl. Electrochem **16**, 422 (1986)
13. A.A. Samarskii, Introduction in theory of difference schemes (in Russian). (Nauka, Moscow, 1971)